

Disappearance of non-trivial net baryon density distribution effect on the rapidity width of Λ in p+p collisions at Large Hadron Collider energies

Nur Hussain and Buddhadeb Bhattacharjee†

Nuclear and Radiation Physics Research Laboratory, Department of Physics,
Gauhati University, Guwahati-781014, India

E-mail: nur.hussain@cern.ch, buddhadeb.bhattacharjee@cern.ch

† Corresponding author

15 December 2024

Abstract. Pseudorapidity distributions of all primary charged particles produced in p+p collisions at various Relativistic Heavy Ion Collider (RHIC) and Large Hadron Collider (LHC) energies using UrQMD-3.4 and PYTHIA8-generated events are presented and compared with the existing results of UA5 and ALICE collaborations. With both the sets of generated data, the variation of rapidity widths of different mesons and baryons of p+p collisions at various Super Proton Synchrotron (SPS) and LHC energies with the rest masses of the studied hadrons are presented. An increase in the width of the rapidity distribution of Λ , similar to heavy-ion data, could be seen from SPS to the highest LHC energies when the entire rapidity space is considered. However, at LHC energies, in the rapidity space where $B - \bar{B} = 0$, the shape of the rapidity distribution of Λ takes the same Gaussian shape as that of $\bar{\Lambda}$ and the widths of both the distributions become same confirming the disappearance of net baryon density distribution effect on the rapidity width of Λ . Further, a multiplicity dependent study confirms that the jump in the width of the rapidity distribution of Λ disappears for the highest multiplicity class at LHC energy. This observation confirms that the light flavoured spectator partons play a significant role in Λ production in p+p collisions at LHC energies.

1. Introduction

Estimation of the widths of the rapidity distributions of identified charged particles is of quite significance as they believe to carry a number of information about the dynamics of high-energy nuclear collisions [1–5]. A systematic study on the variation of the widths of the rapidity distributions of various identified particles with their rest masses at different beam rapidities from AGS to SPS energies [3], reveals a jump in the rapidity width of Λ with both UrQMD-generated and available experimental data [4]. The universal mass ordering of the rapidity width of the identified particles [3], seems to get violated at Λ resulting separate mass scaling for mesons and baryons [4]. Such a

jump in the rapidity width of Λ was attributed to the net baryon density distribution effect [4]. Production of Λ (uds) having two leading quarks, and not $\bar{\Lambda}$ ($\bar{u}\bar{d}\bar{s}$) having all produced quarks, is influenced by the net baryon density distribution as a considerable fraction of Λ at these collision energies are due to associate production. Subsequently, when this study was extended to higher SPS, RHIC, and LHC energies, with UrQMD-generated and available experimental results [3,6–8], where the collisions are much more transparent, but $B - \bar{B}$ is still greater than zero, this jump in the width of the rapidity distribution of Λ is yet found to exist and is considered to be a universal feature of heavy-ion collision data from the AGS and SPS to RHIC and LHC energies [5]. Thus the width of the rapidity distribution of Λ produced in heavy-ion collisions is found to have a non-trivial non-kinematic contribution due to its associate production. In A+A collisions, up to the highest available LHC energies, with UrQMD-generated data, a situation could never be reached with $B - \bar{B} = 0$ and thus it could not be ascertained if the rapidity width of Λ is free from net baryon density distribution effect or otherwise if the Λ s are produced through pair production only.

It has been reported in [9] by ALICE collaboration that $\bar{\Lambda}/\Lambda$ ratio becomes unity in p+p collisions at 7 TeV at mid-rapidity. It may, therefore, be expected that for such situation $B - \bar{B}$ would become zero and thus the Λ s are produced through pair production only. Here it is worth mentioning that the colliding protons at the ultra-relativistic energies are considered not only to be composite but also extended objects consisting of many partons, which resembles a situation similar to heavy-ion collisions where the collision ranges from central (high multiplicity) to peripheral (low multiplicity) one [10]. While in A+A collisions, the spectator regions are composed of hadronic matter, in case of p+p collisions the spectators are made up of partonic matter only. As it has been seen in [4,5] for heavy-ion collisions that the spectator hadrons play a significant role in particle production, particularly the Λ production, it would be interesting to see how these spectator partons of p+p collisions play its role in particle production. Thus, multiplicity dependent study on the width of the rapidity distribution of Λ ($\bar{\Lambda}$) produced in p+p collisions at LHC energies could be of quite significance.

It has been claimed in a number of reports [11–13] that UrQMD is quite successful in describing heavy-ion collisions data over a wide range of energies. In [14] it has also been shown that UrQMD is equally successful in describing the experimental results of p+p, Au+Au, and Pb+Pb collisions from 17.3 GeV at the SPS to 1.8 TeV at Fermilab. Further in [5] it has been shown that UrQMD is quite successful in describing the pseudorapidity distributions of all charged particles in Pb–Pb collisions at LHC energies. It is therefore expected that UrQMD could be successfully applied for small system like pp at LHC energies as well. On the other hand, PYTHIA has been found to be quite successful in explaining the p+p experimental results particularly at higher energies like that of LHC [15,16]. In this work an attempt has therefore been made, with UrQMD-3.4 and PYTHIA8 (Monash and 4C tuned) generated p+p events, to estimate the widths of the rapidity distributions of various produced particles including Λ and $\bar{\Lambda}$ at different beam energies to examine how the rapidity width of Λ (and $\bar{\Lambda}$) behave in p+p collisions

for situation for which $B - \bar{B} = 0$. Further, a study on the widths of the rapidity distributions of different hadrons for various multiplicity classes at the highest LHC energy using PYTHIA8 Monash-generated data has been carried out to evaluate the role of spectator partons, particularly on Λ production.

2. MC event generators

For the present study, events were generated using the latest version of Ultra-relativistic Quantum Molecular Dynamics (UrQMD) Monte-Carlo (MC) event generator for p+p collisions at various colliding energies from SPS to the highest LHC energies and the events statistics are presented in Table 1. UrQMD is a many-body microscopic Monte Carlo event generator based on the covariant propagation of color strings, constituent quarks and diquarks with mesonic and baryonic degrees of freedom [14, 17–20]. It includes PYTHIA to incorporate the hard perturbative QCD effects [21, 22]. The current version of the UrQMD model also includes the excitation and fragmentation of color strings, formation and decays of hadronic resonances, and rescattering of particles. On the other hand, PYTHIA, a standalone event generator, consists of a coherent set of physics models, which describes the evolution of high-energy collisions from a few-body hard-scattering processes to a complex multiparticle final state [23, 24]. The present version of the PYTHIA model contains a library of hard processes, models for initial and final state parton showers, multiple parton-parton interactions, string fragmentation, particle decays and beam remnant [24, 25]. The available high precision experimental data, allow detailed model comparisons and motivate the effort on model development and tuning of the existing models towards more precise predictions. One of the dedicated tunings of PYTHIA8 event generator is PYTHIA8 4C, which is used to predict the Run 1 LHC data and the modified parameters are reported in [26]. As reported in [27], the latest PYTHIA8 version is tuned with Monash with the present available LHC data of Run 2. For the present study, we also generated 50 to 80 million p+p inelastic events at each studied energies using PYTHIA8 4C and Monash tuning.

3. Results

In our earlier work [5], it has been shown that UrQMD-3.4-generated (pseudo)rapidity distributions of produced particles show a good agreement with the experimental results at all the SPS, RHIC, and LHC energies for Au+Au and Pb+Pb systems. With the present sets of generated data, pseudorapidity distributions of all primary charged particles are compared with the various existing experimental results of p+p collisions of UA5 and ALICE collaborations. Pseudorapidity distributions of all primary charged particles using UrQMD-3.4 and PYTHIA8-generated events of p+p collisions at $\sqrt{s} = 53$ (only UrQMD), 200, 546, and 900 GeV are compared with the results of UA5 collaboration [28] and is shown in the left panel of Fig. 1. Though the MC data reproduces well the shape of the experimental pseudorapidity distributions

Table 1. Event statistics of UrQMD-3.4-generated p+p collision data at all the studied energies.

Energy (GeV) \sqrt{s} (E_{lab})	Events (million)	$\pi^- \times 10^7$	$K^- \times 10^6$	$\bar{p} \times 10^5$	$\phi \times 10^5$	$\Lambda \times 10^6$	$\Xi^- \times 10^4$	$\Omega^- \times 10^2$
(20)	67.04	4.42	1.13	1.38	0.26	2.13	0.56	0.26
(30)	134.43	11.67	4.20	8.42	1.13	5.76	3.43	7.93
(40)	46.87	4.87	2.09	5.27	0.61	2.40	2.16	8.25
(80)	61.53	9.38	5.33	17.40	1.96	4.44	7.33	49.85
(158)	53.62	11.05	7.38	26.67	3.25	4.91	11.52	103.13
19.6	42.91	9.74	6.80	25.14	3.19	4.21	10.08	103.22
53	31.00	12.35	10.63	45.23	7.67	4.45	18.85	222.82
62.4	31.71	13.48	11.84	51.53	9.17	4.75	21.04	247.80
130	43.34	23.25	22.03	106.03	22.84	7.645	38.85	400.50
200	51.71	31.70	31.32	161.38	38.62	10.06	54.29	450.09
546	48.41	42.34	45.42	288.96	73.60	12.71	76.95	279.38
900	113.91	119.54	131.3	862.67	223.43	33.80	220.76	580.82
2760	90.26	147.04	166.80	1111.75	365.66	36.56	279.12	714.76
5020	72.28	142.78	163.24	1091.39	286.23	33.96	274.19	717.36
7000	42.68	93.00	106.88	713.95	187.40	21.70	179.43	475.75
13000	29.60	76.25	88.12	589.00	154.67	17.28	148.34	395.27

of UA5 collaboration, around mid-rapidity, the models somewhat under-predict the experimental values at all the studied energies of UA5 collaboration. However, in the right panel of Fig. 1, all sets of generated data (UrQMD-3.4, PYTHIA8 4C, and PYTHIA8 Monash) at $\sqrt{s} = 900$ GeV show a better agreement with the experimental results of ALICE collaboration [15, 16].

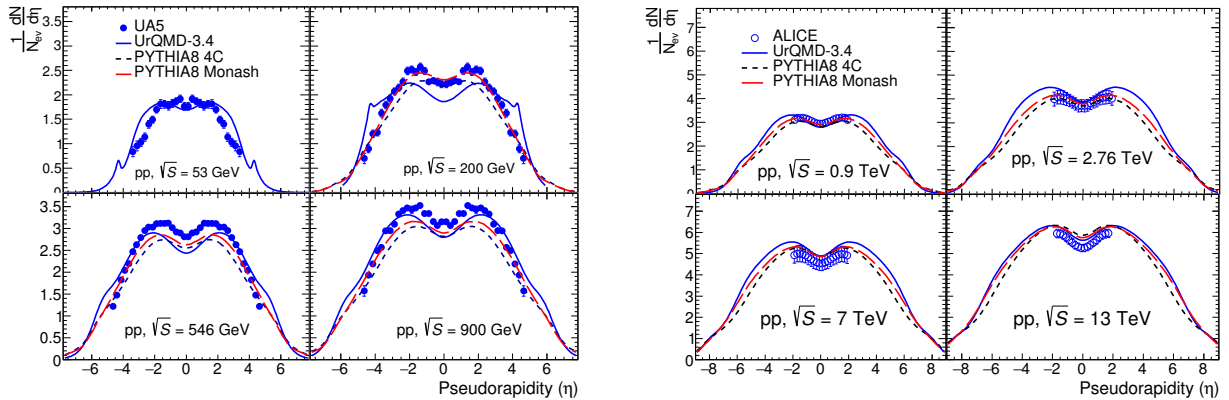


Figure 1. Comparison of pseudorapidity distributions of all primary charged particles with UrQMD-3.4, PYTHIA8 4C, and PYTHIA8 Monash generated events in p+p collisions at $\sqrt{s} = 53, 546, 200,$ and 900 GeV with UA5 collaboration [28] (left panel), and at $\sqrt{s} = 0.9, 2.76, 7,$ and 13 TeV with ALICE collaboration [15, 16] (right panel). The blue solid and open circular symbols represent the experimental results of UA5 and ALICE collaborations respectively, whereas blue solid, black small dashed and red long dashed lines represent the results of UrQMD-3.4, PYTHIA8 4C, and PYTHIA8 Monash generated data respectively.

It may be mentioned here that the cause of observed small difference in the pseudorapidity distributions of UA5 and ALICE collaborations (e.g., at $\sqrt{s} = 900$ GeV) is discussed in [15] and is attributed to the facts that – (i) UA5 collaboration used a $1/M_x$ variation of single diffractive cross sections [29] and (ii) inconsistent UA5 internal data as discussed in [30]. It may further be noted that, while the comparison of PYTHIA8 4C- and PYTHIA8 Monash-generated pseudorapidity distributions of all primary charged particles with experimental data of ALICE collaboration could also be found in [15,16], UrQMD-3.4-generated pseudorapidity distributions at LHC energies, to the best of our knowledge, have been compared for the first time in this report. From Fig. 1 it is clearly seen that PYTHIA8 Monash tuned pseudorapidity distribution of primary charged particles lies between PYTHIA8 4C and UrQMD-3.4 predicted results. Considering the fact that all the three sets of model-predicted pseudorapidity distributions are in good agreement with the experimental results of appropriate energies, further analysis is carried out with all the three, i.e., UrQMD-3.4, PYTHIA8 4C, and PYTHIA8 Monash model-generated data.

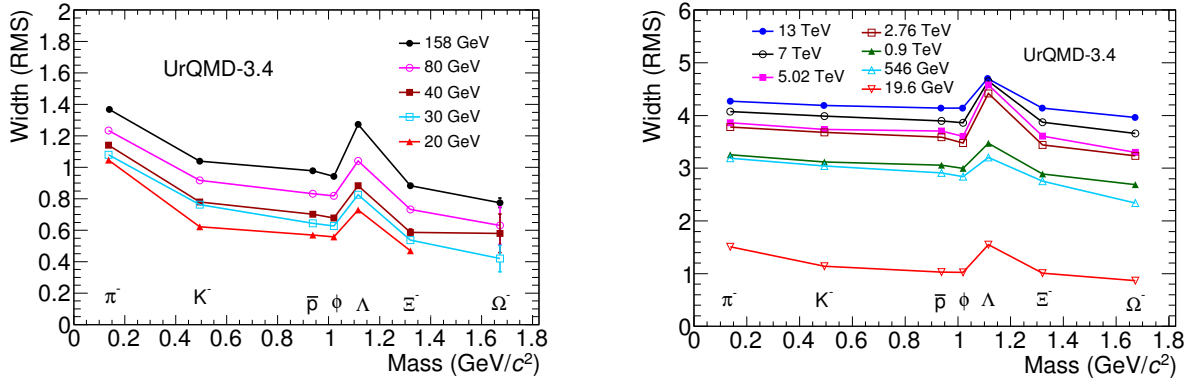


Figure 2. Widths of the rapidity distributions of various produced particles as a function of their rest masses in p+p collisions at all the SPS energies (left panel), lower RHIC, and all the LHC energies (right panel) using UrQMD-3.4-generated events for $|y| \leq 6.5$ (excluding the extreme peaks of the rapidity distribution of Λ). The different markers with different colors correspond to various beam energies. The solid lines with different colors are to guide the eyes only.

UrQMD-3.4- and PYTHIA8 (4C and Monash)-generated rapidity distributions of π^- , K^- , \bar{p} , ϕ , Λ , Ξ^- , and Ω^- at all the studied energies for p+p collisions are parameterized by the following double Gaussian function [4, 8]:

$$\frac{dN}{dy} \propto \left(e^{-\frac{(y-\bar{y})^2}{2\sigma^2}} + e^{-\frac{(y+\bar{y})^2}{2\sigma^2}} \right), \quad (1)$$

where the symbols have their usual significance. Using this fitting function, widths of the rapidity distributions of generated data of all the studied hadrons are estimated and listed in Tables 2 and 3. The variation of the rapidity widths of various mesons and

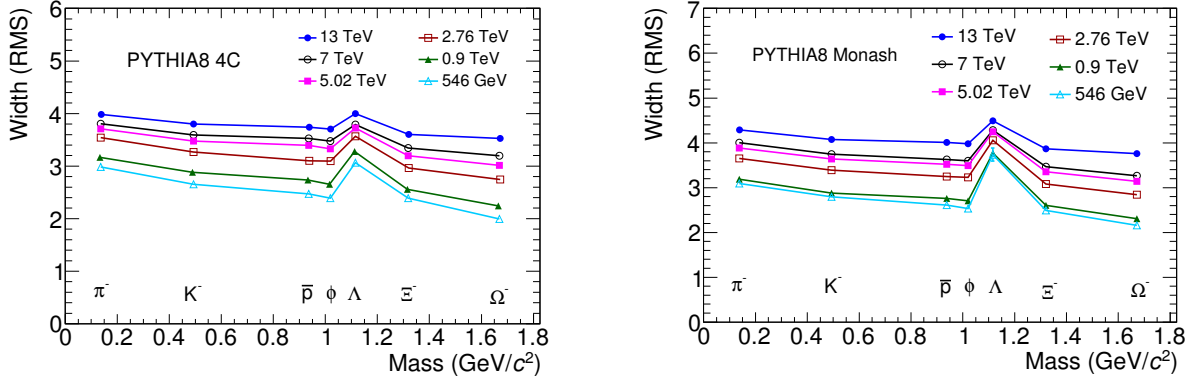


Figure 3. Widths of the rapidity distributions of various produced particles as a function of their rest masses in p+p collisions from $\sqrt{s} = 0.546$ TeV to 13 TeV using PYTHIA8 4C (left panel) and PYTHIA8 Monash (right panel) generated inelastic events for $|y| \leq 7$ (excluding the extreme peaks of the rapidity distribution of Λ). The different markers with different colors correspond to various beam energies. The solid lines with different colors are to guide the eyes only.

Table 2. Widths of the rapidity distributions of all the studied hadrons with UrQMD-3.4-generated p+p events at all the SPS, lower RHIC, and all the LHC energies. At LHC energies, rapidity widths of Λ s are estimated using double Gaussian function excluding the extreme two peaks, whereas rapidity widths estimated using triple Gaussian function including all the three peaks are shown in the parentheses.

Energy \sqrt{s} (E_{lab})	π^-	K^-	\bar{p}	ϕ	Λ	Ξ^-	Ω^-
(20 GeV)	1.045 ± 0.001	0.622 ± 0.002	0.570 ± 0.003	0.558 ± 0.011	0.728 ± 0.001	0.468 ± 0.017	-
(30 GeV)	1.078 ± 0.001	0.762 ± 0.002	0.644 ± 0.003	0.627 ± 0.007	0.826 ± 0.001	0.536 ± 0.009	0.419 ± 0.084
(40 GeV)	1.115 ± 0.002	0.779 ± 0.006	0.701 ± 0.008	0.678 ± 0.017	0.883 ± 0.002	0.586 ± 0.022	0.590 ± 0.240
(80 GeV)	1.230 ± 0.001	0.916 ± 0.007	0.832 ± 0.005	0.818 ± 0.014	1.040 ± 0.002	0.731 ± 0.014	0.630 ± 0.120
(158 GeV)	1.369 ± 0.001	1.039 ± 0.002	0.979 ± 0.003	0.942 ± 0.008	1.273 ± 0.001	0.883 ± 0.010	0.774 ± 0.029
19.6 GeV	1.414 ± 0.001	1.137 ± 0.002	1.031 ± 0.002	0.993 ± 0.005	1.352 ± 0.001	0.963 ± 0.006	0.833 ± 0.017
546 GeV	3.174 ± 0.002	3.043 ± 0.007	2.913 ± 0.007	2.842 ± 0.013	3.204 ± 0.024	2.754 ± 0.035	2.337 ± 0.014
900 GeV	3.254 ± 0.002	3.122 ± 0.006	3.056 ± 0.002	2.989 ± 0.014	3.487 ± 0.036	2.909 ± 0.042	2.461 ± 0.093
2.76 TeV	3.766 ± 0.001	3.681 ± 0.001	3.587 ± 0.002	3.479 ± 0.002	4.417 ± 0.014	3.444 ± 0.007	3.237 ± 0.030
5.02 TeV	3.861 ± 0.002	3.735 ± 0.002	3.704 ± 0.002	3.604 ± 0.004	4.583 ± 0.028	3.611 ± 0.015	3.301 ± 0.065
7 TeV	4.060 ± 0.001	3.987 ± 0.001	3.897 ± 0.001	3.860 ± 0.003	4.650 ± 0.013	3.871 ± 0.010	3.662 ± 0.043
13 TeV	4.267 ± 0.001	4.178 ± 0.001	4.138 ± 0.001	4.129 ± 0.003	4.690 ± 0.009	4.140 ± 0.012	3.953 ± 0.051
					(4.55 \pm 0.019)		
					(5.091 \pm 0.003)		
					(5.152 \pm 0.008)		
					(5.158 \pm 0.003)		
					(5.180 \pm 0.003)		

Table 3. Widths of the rapidity distributions of all the studied hadrons with PYTHIA8 Monash-generated inelastic p+p events from 564 GeV to the top LHC energies. At LHC energies, rapidity widths of Λ s are estimated using double Gaussian function excluding the extreme two peaks, whereas rapidity widths estimated using triple Gaussian function including all the three peaks are shown in the parentheses.

Energy \sqrt{s} (E_{lab})	π^-	K^-	\bar{p}	ϕ	Λ	Ξ^-	Ω^-
546 GeV	3.078 ± 0.001	2.796 ± 0.002	2.609 ± 0.001	2.533 ± 0.003	3.738 ± 0.144	2.490 ± 0.007	2.156 ± 0.020
900 GeV	3.174 ± 0.001	2.876 ± 0.001	2.761 ± 0.001	2.705 ± 0.002	3.770 ± 0.044 (4.352 ± 0.010)	2.606 ± 0.005	2.307 ± 0.017
2.76 TeV	3.647 ± 0.001	3.390 ± 0.001	3.248 ± 0.001	3.227 ± 0.003	4.056 ± 0.023 (4.655 ± 0.007)	3.080 ± 0.006	2.845 ± 0.021
5.02 TeV	3.880 ± 0.001	3.639 ± 0.001	3.520 ± 0.001	3.493 ± 0.004	4.248 ± 0.015 (4.826 ± 0.006)	3.352 ± 0.005	3.143 ± 0.020
7 TeV	3.985 ± 0.001	3.748 ± 0.001	3.631 ± 0.001	3.599 ± 0.002	4.283 ± 0.011 (4.925 ± 0.005)	3.468 ± 0.005	3.267 ± 0.017
13 TeV	4.291 ± 0.002	4.075 ± 0.002	4.007 ± 0.002	3.981 ± 0.005	4.489 ± 0.011 (5.085 ± 0.006)	3.864 ± 0.009	3.762 ± 0.037

baryons as a function of their rest masses at all the SPS, lower RHIC, and all the LHC energies for the rapidity space $|y| < 7$ are shown in Figs. 2 and 3.

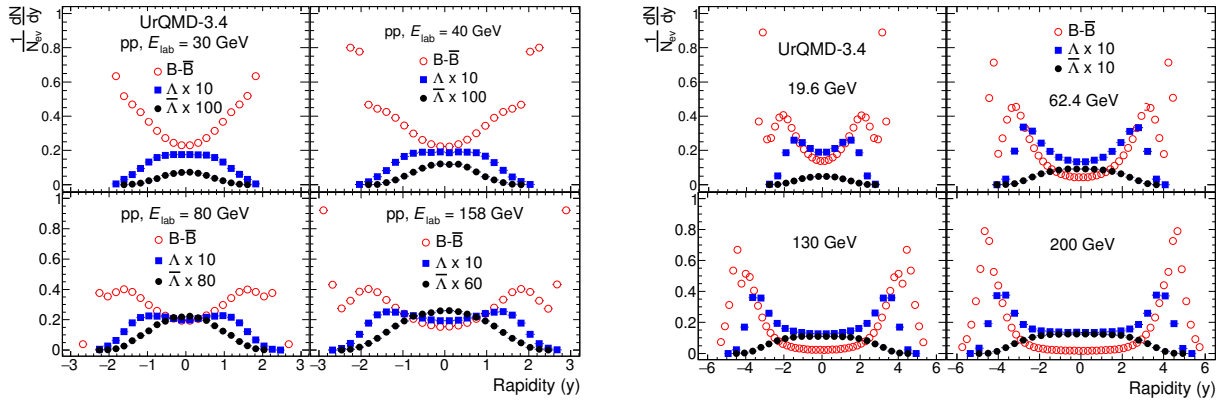


Figure 4. Distributions of $B - \bar{B}$, Λ , and $\bar{\Lambda}$ over the entire rapidity space using UrQMD-3.4-generated events in p+p collisions at various SPS (left panel) and RHIC (right panel) energies. The open circular, filled square, and filled circular symbols represent the rapidity distributions of $B - \bar{B}$, Λ , and $\bar{\Lambda}$ respectively.

It could be readily seen from Figs. 2 and 3 that, as reported in [4, 5] for heavy-ion collisions from AGS to LHC energies, a similar jump in the rapidity width of Λ does exist also in the case of minimum bias p+p collisions from low SPS to the highest LHC energies for both UrQMD-3.4 and PYTHIA8 (4C and Monash tuned) models generated data. Such an increase in the width of the rapidity distribution of Λ (uds) and not $\bar{\Lambda}$ ($\bar{u}\bar{d}\bar{s}$) [3], was attributed to the dependence of Λ production on net baryon density distribution or otherwise on associate production of Λ [4, 5]. In p+p collisions, as shown in the left panel of Fig. 4, the net baryon density is found to be maximum at extreme rapidities even at low SPS energies and minimum but not zero at zero-rapidity.

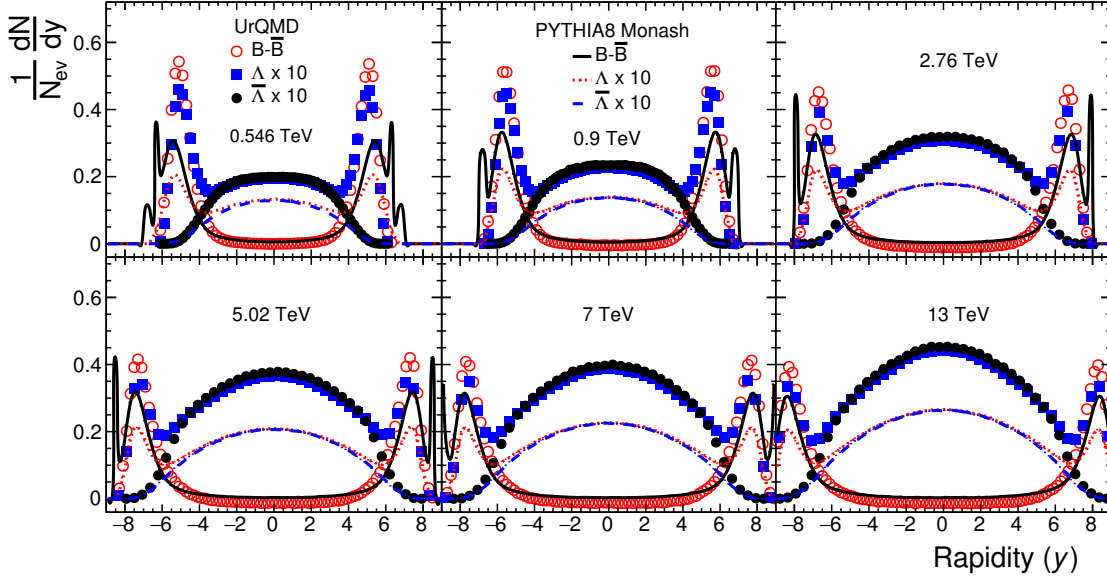


Figure 5. Distributions of $B - \bar{B}$, Λ and $\bar{\Lambda}$ over the entire rapidity space using UrQMD-3.4 and PYTHIA8-generated events in p+p collisions at various energies of UA5 and ALICE collaborations. The open circular, filled square, and filled circular symbols represent the UrQMD-3.4-generated rapidity distributions of $B - \bar{B}$, Λ , and $\bar{\Lambda}$ respectively. The black solid, red dotted, and blue dashed lines represent PYTHIA8 Monash-generated rapidity distributions of $B - \bar{B}$, Λ , and $\bar{\Lambda}$ respectively.

Unlike in heavy-ion collisions, the spectator regions of p+p collisions consist of partonic rather than hadronic matter and therefore the observed maximum net baryon density at extreme rapidity space in p+p collisions are not due to the leading hadrons but due to the hadrons produced out of leading partons (partons of the spectators). As the collision energy increases, the minimum value of the net baryon density decreases reaching zero at lower LHC energies ($\sqrt{s} = 0.9$ TeV) (Figs. 4 and 5). Further, with the increase of the collisions energies, the minimum net baryon density region extends over more rapidity space around mid-rapidity. At SPS and RHIC energies, $B - \bar{B} > 0$ at all rapidity space and thus the rapidity distribution of Λ follows the net baryon density distribution pattern resulting a jump in the rapidity width vs. mass plot. At LHC energies, $B - \bar{B} = 0$ over a wide rapidity range and the rapidity distributions of both Λ and $\bar{\Lambda}$ follow the same Gaussian pattern over the rapidity space for which $B - \bar{B} = 0$. Thus in p+p collisions at LHC energies, the rapidity distributions of Λ become independent of net baryon density distribution pattern and resemble exactly that of $\bar{\Lambda}$ over the rapidity space for which $B - \bar{B} = 0$. Thus, in a scenario where net baryon density is zero, the widths of rapidity distributions of Λ and $\bar{\Lambda}$ become equal or in other words, the rapidity width of Λ does not exhibit any non-trivial (non-kinematic) contribution for a situation for which $B - \bar{B} = 0$.

To have a cross-check on the above observation, another 80 million pp inelastic events were generated at the highest LHC energies ($\sqrt{s} = 13$ TeV) using PYTHIA8

Monash tuned event generator. The rapidity distribution of Λ , $\bar{\Lambda}$ and net baryon density, and the variation of the widths of the rapidity distribution of various hadrons as a function of the rest masses have plotted in Figs. 6 and 7 respectively.

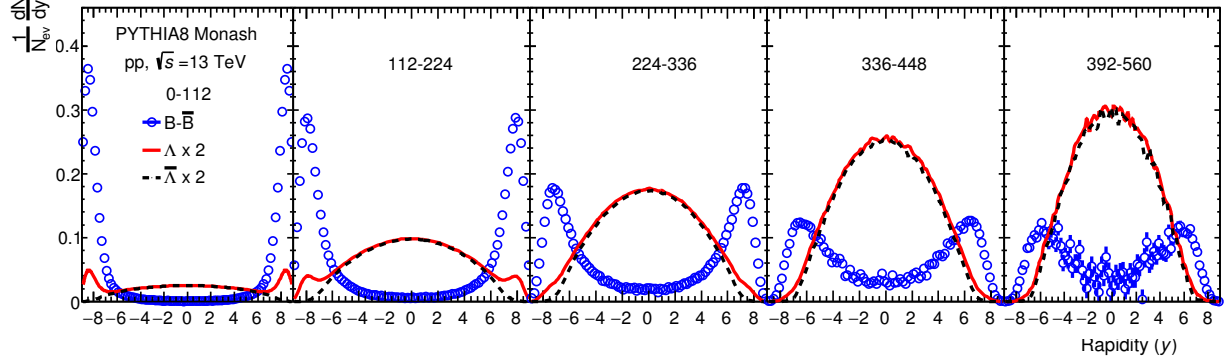


Figure 6. Width of the rapidity distributions of $B - \bar{B}$, Λ and $\bar{\Lambda}$ in p+p collisions at $\sqrt{s} = 13$ TeV for different multiplicity classes using PYTHIA8 Monash-generated inelastic events. The open blue circular, red dashed and black dotted markers represent the rapidity distributions of $B - \bar{B}$, Λ and $\bar{\Lambda}$ respectively.

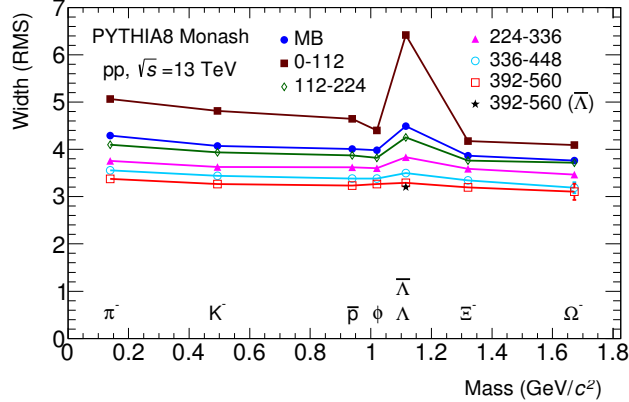


Figure 7. Width of the rapidity distributions as a function of their rest masses for various multiplicity classes in pp collisions at $\sqrt{s} = 13$ TeV with PYTHIA8 Monash-generated inelastic events. Different marker symbols represent the widths of the rapidity distributions of various hadrons for different multiplicity classes. The star marker symbol represents the rapidity width of $\bar{\Lambda}$ for the multiplicity class of 392-560.

It is evident from Fig. 6 that the net baryon density, which arises due to the difference in produced hadrons and their anti-particles created out of spectators' partons, i.e., beam remnants, is more in the extreme rapidity regions for low multiplicity classes. A non-zero value of $B - \bar{B}$ at extreme rapidity for low multiplicity pp collisions suggests the presence of more quarks than antiquarks in the extreme rapidity regions favouring the production of more baryons than antibaryons. Thus, at LHC energies, the beam protons, which are considered to be extended balls of partons seems to be composed of

more quarks than antiquarks favouring baryon asymmetry at extreme rapidity regions. The hadron (particularly Λ) production in such low multiplicity p+p events, has a substantial contribution from the partons of the spectators [10], which could be the main reason of the increase in the width of the rapidity distribution of Λ as shown in Fig. 7. Further, it is clearly seen from Fig. 7 that the width of the rapidity distributions of all the studied hadrons decreases with increasing multiplicity or otherwise centrality and for the highest multiplicity class when there is no beam remnants, the jump in the rapidity width of Λ almost disappears. Therefore, for the most central collisions, in absence of spectator, the production of Λ s becomes independent of the nature of the net baryon density distribution and hence, the width of the rapidity distribution of Λ becomes the same as that of $\bar{\Lambda}$ (Fig. 8). Such observation reveals that in high multiplicity p+p collisions, where the spectator part is either absent or negligible, the Λ s might be pair produced.

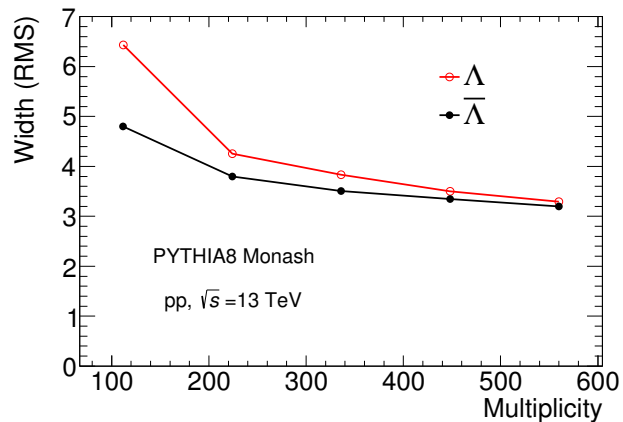


Figure 8. Widths of the rapidity distributions of Λ and $\bar{\Lambda}$ as a function of charged particle multiplicity in p+p collisions at $\sqrt{s} = 13$ TeV using PYTHIA8 Monash-generated inelastic events. The open and solid markers represent the widths of Λ and $\bar{\Lambda}$ respectively.

4. Summary

In this work UrQMD-3.4 and PYTHIA8-generated pseudorapidity distributions of all primary charged particles of p+p collisions are compared with the existing experimental results of UA5 and ALICE collaborations which show good agreement between model generated and experimental results for the studied energies. An increase in the rapidity width of Λ , as observed in heavy-ion data [5], could be seen with the generated data of p+p collisions as well at all the SPS energies. When the study is extended to RHIC and LHC energies, a similar increase in the rapidity width of Λ could be observed for the consideration of full rapidity space indicating that the increase in the rapidity width of Λ is a general characteristic of both p+p and A+A collisions from SPS to RHIC

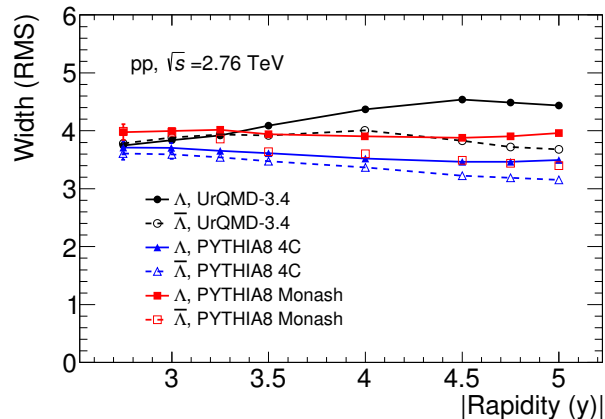


Figure 9. Widths of the rapidity distributions as a function of rapidity window of Λ and $\bar{\Lambda}$ using UrQMD-3.4-generated events in p+p collisions at $\sqrt{s} = 2.76$ TeV. The solid circle, triangle, and square symbols with different colors represent the widths of the rapidity distributions of Λ for UrQMD-3.4, PYTHIA8 4C, and PYTHIA8 Monash respectively, whereas the corresponding open marker symbols represent the widths of the rapidity distributions of $\bar{\Lambda}$.

and LHC energies. For p+p collisions at various RHIC and LHC energies, even though $B - \bar{B} = 0$ at the mid-rapidity, a small non-zero $B - \bar{B}$ at higher rapidity regions is responsible for the observed jump in the rapidity width of Λ . A plot of widths of the rapidity distributions of Λ and $\bar{\Lambda}$ as a function of rapidity window (Fig. 9), shows that at the rapidity windows for which $B - \bar{B} = 0$, the widths of rapidity distributions of Λ and $\bar{\Lambda}$ become same. Also, widths of the rapidity distributions of Λ and $\bar{\Lambda}$ become the same for high multiplicity p+p events over the entire rapidity regions (Fig. 8), where the system has the maximum probability of multiple parton interactions. Such observations suggest that at LHC energies at and around mid-rapidity as well as for high multiplicity p+p events over the entire rapidity region, Λ and $\bar{\Lambda}$ are mostly pair produced.

Acknowledgments

The financial assistance of Department of Science and Technology (DST), Government of India through the project No. SR/MF/PS-01/2014-GU (C) is thankfully acknowledged.

References

- [1] J. L. Klay *et al* (E895 Collaboration), Phys. Rev. Lett. **88**, 102301 (2002).
- [2] B. Mohanty and Jan-e Alam, Phys. Rev. C **68**, 064903 (2003).
- [3] C. Blume (NA49 Collaboration), J. Phys. G: Nucl. Part. Phys. **31** S685–S691 (2005).
- [4] K. Dey and B. Bhattacharjee, Phys. Rev. C **89**, 054910 (2014).
- [5] N. Hussain and B. Bhattacharjee, Phys. Rev. C **96**, 024903 (2017).
- [6] S. V. Afanasiev *et al* (NA49 Collaboration), Phys. Rev. C **66**, 054902 (2002).
- [7] C. Alt *et al* (NA49 Collaboration), Phys. Rev. C **78**, 044907 (2008).
- [8] C. Alt *et al* (NA49 Collaboration), Phys. Rev. C **78**, 034918 (2008).

- [9] E. Abbas *et al* (ALICE collaboration), *Eur. Phys. J. C* **73**:2496 (2013).
- [10] T. Sjostrand and M. van Zijl, *Phys. Rev. D* **36**, 2019 (1987).
- [11] S. A. Bass *et al*, *Phys. Rev. Lett.* **81**, 4092 (1998).
- [12] M. Bleicher *et al*, *Phys. Lett. B* **447**, 227 (1999).
- [13] M. Bleicher *et al*, *Phys. Lett. B* **435**, 9 (1998).
- [14] M. Mitrovski, T. Schuster, G. Graf, H. Petersen, and M. Bleicher, *Phys. Rev. C* **79**, 044901 (2009).
- [15] J. Adam *et al* (ALICE collaboration), *Eur. Phys. J. C* **77**:33 (2017).
- [16] J. Adam *et al* (ALICE collaboration), *Phys. Lett. B* **753** 319-329 (2016).
- [17] H. Petersen, M. Bleicher, S. A. Bass, and H. Stoecker, arXiv:0805.0567 [hep-ph].
- [18] B. Andersson, G. Gustafson, and B. Nilsson-Almqvist, *Nucl. Phys. B* **281**, 289 (1987).
- [19] B. Nilsson-Almqvist and E. Stenlund, *Comput. Phys. Commun.* **43**, 387 (1987).
- [20] T. Sjostrand, *Comput. Phys. Commun.* **82**, 74 (1994).
- [21] M. Bleicher *et al*, *J. Phys. G: Nucl. Part. Phys.* **25**, 1859 (1999).
- [22] S. A. Bass *et al*, *Prog. Part. Nucl. Phys.* **41**, 255 (1998).
- [23] T. Sjostrand, S. Mrenna and P. Skands, *JHEP* 05 026 [hep-ph/0603175] (2006).
- [24] T. Sjostrand, S. Mrenna and P. Skands, *Comput. Phys. Commun.* **178**, 852–867 (2008).
- [25] Torbjorn Sjostrand *et al*, *Comput. Phys. Commun.* **191** 159-177 (2015).
- [26] Richard Corke and Torbjorn Sjostrand, *JHEP* 03 032 (2011).
- [27] P. Skands, S. Carrazza and J. Rojo, *Eur. Phys. J. C* **74**:3024 (2014).
- [28] G. J. Alner *et al* (UA5 Collaboration), *Z. Phys. C* **33**: 1–6 (1988).
- [29] A.B. Kaidalov, M.G. Poghosyan, *Proceedings, 13th International Conference, Blois Workshop, CERN, Geneva, Switzerland, 29 June–3 July 2009*, pp. 91-98 (2009). arXiv:0909.5156 [hep-ph].
- [30] M. Poghosyan, arXiv:1005.1806 [hep-ph].